Sensors and Materials, Vol. 33, No. 9 (2021) 3317–3324
MYU Tokyo

S & M 2691

Parameter Matching for 3D Images by a Real 3D Display System with Sensors

Chong Zeng,[1,2] Yue Wu,[2] Jiali Chen,[1] Tao Zan,[1]
Hsien-Wei Tseng,[1*] and Chun-Chi Chen[3**]

[1]College of Mathematics and Information Engineering, Longyan University,
No. 1 North Road, Dong Xiao Town, Long Yan City 369000, China
[2]School of Informatics, University of Leicester,
University Road, Leicester LE1 7RH, UK
[3]School of Life Sciences, Longyan University, Longyan, Fujian 364012, China

(Received March 26, 2021; accepted September 2, 2021)

Keywords: real 3D display, high-speed, holographic, DMD, DLP, CMOS sensor

In this paper, we describe several key problems in the design of a real 3D display system with sensors (RDSS) and details of matching the parameters to generate 3D images. We also illustrate the feasibility of using light fields to reconstruct 3D images. Additionally, we propose a real 3D display based on optical field reconstruction that also solves the problems of fuzzy images and low mechanical stability caused by the scattering characteristics in an optical field display. We acquire images through sensors and project them to a high-speed rotating mirror through digital light processing (DLP) after computer processing. At the same time, DLP is used to project images to the horizontal space, so that they can be observed by human eyes without auxiliary equipment. We find the best parameters for achieving a clear and stable image by comparing different experimental data. The matching parameters provided in this study can greatly reduce the cost of real 3D display systems that are easily usable and realizable and can be widely used in advertising, exhibitions, and other applications.

1. Introduction

Early research on 3D displays, such as stereoscopic and autostereoscopic displays, provided only the illusion of 3D perception. In contrast, with the rapid development of new 3D display technologies, it is now possible to experience real 3D displays, such as integral imaging, volumetric holography, and light field displays.(1) Stereoscopic and autostereoscopic 3D displays are affected by flicker induced by temporal multiplexing and crosstalk (information leaking from one eye view to the other), which not only seriously reduces the perceived image quality, but also affects the fusion of two images.(2) A real 3D display remedies the defects of stereoscopic 3D displays by integrating the intermittent information around the visual system through the high-frame-rate output and reducing the interocular crosstalk to achieve a real 3D display effect.(2) The real 3D display system with sensors (RDSS) developed in this study is based on the reduction of interocular crosstalk.

*Corresponding author: e-mail: hsienwei.tseng@gmail.com
**Corresponding author: e-mail: kennath1980@gmail.com
https://doi.org/10.18494/SAM.2021.3401

ISSN 0914-4935
https://myukk.org/

This paper presents a 360° floating light field display system that can display floating 3D images in the air, which can be viewed from any angle with the naked eye without wearing any accessories. First, we introduce the components of the system, which consists of a CMOS image sensor (CIS), an IR radiation sensor (IRS), an industrial-grade optical projection module for digital light processing (DLP), a stainless steel directional scattering mirror (DSM), a high-speed rotating stainless steel disc, and a high-speed mini-motor. Then we discuss the RDSS, which can provide continuous views with vertical and horizontal parallax by generating 3D images with vertical viewing angles of up to 12.5° and horizontal viewing angles of up to 360° with image sizes greater than 20 cm. Additionally, the DSM adopts an adjustable light shaping diffuser (ALSD) to reduce specular scattering, which can greatly improve the clarity of the 3D display. In addition, we discuss the problems we encountered, such as the motor vibration problem and the DSM barycenter point finding problem. Finally, we compare the experimental data obtained under various conditions and environments to obtain the best matching parameters for the clearest 3D display.

2. Related Works

In recent years, volumetric displays have occupied the mainstream of research on real 3D displays. In 2018, Smalley *et al.*[3] developed a free-space volumetric display that takes advantage of visual persistence. Its basic principle is to generate 10 μm image points in free space to generate full-color graphics by photophoretic optical trapping. In the following year, Hirayama *et al.*[4] proposed a floating volumetric display (multimodal acoustic trapping display) adopting acoustic holography as a single operating principle, which is characterized by the simultaneous transmission of auditory, visual, and tactile content. Additionally, emerging glasses-free tabletop 3D displays float virtual 3D objects on a flat tabletop surface with a 360° view.[5–7] Although holography displays are rarely used for civil purposes because of their high cost,[8] with most of them used for art exhibitions[9] and commercial performances,[10] the autostereoscopic light field display presented by Jones *et al.*[11] is highly practical and easy to operate.

3. Proposed Real 3D Display System

3.1 Structure and principle of the RDSS

The RDSS is based on the human visual retention characteristic (0.1–0.4 s).[2] To reduce the problem of persistent display (human eyes observing a new frame of an image while the previous frame is still visible) caused by crosstalk, this system adopts a high-speed projector to project an object and integrates intermittent information around the visual system, thus reducing the influence of crosstalk, reconstructing the light field information, and finally realizing a real 3D floating display. In addition, the visual environment of the system should be dark, because the visual residual effect is related to brightness, that is, the greater the brightness, the longer the effect.[12]

The system, whose structure is shown in Fig. 1, operates as follows. First, the image sensor senses objects and transmits them to a highly sensitive digital camera with a CMOS sensor, which is used to obtain a depth cue and light field information of the desired display object, then the sensor transmits them to the computer. Then the computer performs 3D modeling on the sensing object, thus obtaining the 3D stereoscopic model and the angle section. The source images are then sent to an industrial-grade high-speed projector and projected synchronously directly below the DSM. A key requirement is that the center point of the optical axis of the high-speed projector coincides with the center point of the scatterer's rotating barycenter. At the same time, the DSM is driven by a rotating mechanism consisting of a high-speed mini-motor and a rotating shaft to spin at high speeds and scatter light. Finally, we adjust the number and speed of projected images and the speed of the motor to make the parameters match, so as to achieve the optimal efficiency and effect of the floating 3D display.

3.2 Sensors in the RDSS

(1) CIS

An image sensor detects optical images and converts them into electronic signals.[13] Early image sensors used analog signals. Nowadays, image sensors are mainly divided into two types: charge-coupled device (CCD) sensors and CMOS active pixel sensors. The CIS is a type of active pixel sensor using a CMOS semiconductor. There are corresponding circuits for each photoelectric sensor to convert light energy directly into voltage. Unlike a CCD, it does not involve signal charges.[14–17]

(2) IR sensor

This is composed of an IR data processor and an IR transceiver. The IR transceiver is composed of IR tubes, which are assembled in the transceiver and consist of a transmitter and receiver.[18,19] When an object produces emission in the IR range, the IR data operation processing unit can locate the object according to the status of the IR tubes and transmit it to the signal processing unit through the terminal controller.[20–23] The signal processing unit processes the image and transmits it to a high-speed projector.[24]

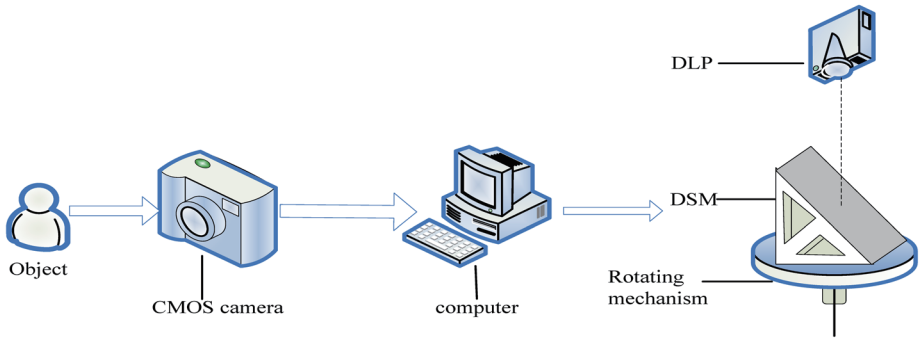

Fig. 1. (Color online) Structure of the RDSS.

3.3 Structure and principle of the DSM

The DSM consists of an ALSD, a stainless steel mirror, and an acrylic triangular bracket, as shown in Fig. 1. The DSM is fixed on a circular turntable at an angle of 45° from the horizontal direction. When the light hits the mirror, the reflected spot area is very small. When the light hits the scatterer, the area of the reflected light spot becomes larger, thus increasing the field angle range.[25] Therefore, the ALSD is adopted to spread the scattering range, so as to increase the field of view angle and enable the image to be observed from different positions over an angle of 360°. Figure 2(a) shows the scattering characteristics of the DSM in the horizontal direction. The ALSD limits the horizontal light to a very small angle α, which is similar to direct reflection, to improve the accuracy of the horizontal reconstruction of the light field. Correspondingly, Fig. 2(b) shows the scattering characteristics of the DSM in the vertical direction. The ALSD scatters light over the maximum angle β in the vertical direction, which is similar to diffusion, so that the observer can observe images with a larger vertical range. To enable the observer to observe the image clearly, the system adopts the ALSD with an angle of 60° in the vertical direction and an angle of 1° in the horizontal direction to improve the scattering performance.

As shown in Fig. 3, the image to be projected is selected according to the angle θ, and Eq. (1) gives the number of projection cross-sectional images v.

$$v = 360/\theta \tag{1}$$

For a motor speed of μ revolutions per minute (rpm), a time of $60/\mu$ s will be required for each rotation of the motor. According to the principle of the 3D display, for every rotation of the DSM disk, the DLP must project the 3D cross section v times. For the frame rate of the DLP of δ, we have

$$\delta = v \times (\mu/60). \tag{2}$$

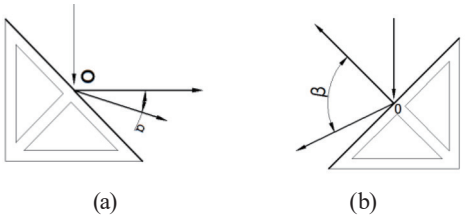

Fig. 2. Principle of the DSM. (a) Horizontal characteristic. (b) Vertical characteristic.

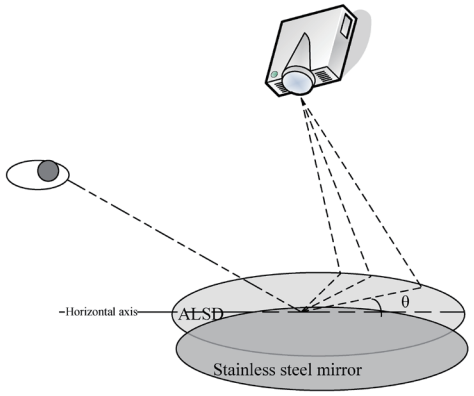

Fig. 3. (Color online) Schematic of the ALSD.

4. Experiments and Discussion

Employing the principle of the 3D image reproduction of the light field, we design a real 3D display device, which includes a projector frame, a protection frame, a rotation frame, and a high-speed mini-motor. Specifically, the moving frame of the projector is composed of a T-shaped bracket and an L-shaped slide rail group made of European standard 3030 aluminum, which can make the projector move up and down and back and forth to adjust the size of the display image. The imaging display platform is made of 12 pieces of aluminum assembled into a rectangular frame structure, with acrylic panels added around for protection. Also, a 10-mm-thick stainless steel plate is installed in the middle to affix the motor and act as a weight in the system. The rotating mirror frame is composed of an acrylic triangular bracket, a stainless steel mirror, and a stainless steel turntable. Additionally, the specific parameter values of the RDSS framework are obtained by SolidWorks® 3D modeling.[26] The rotating disk has a diameter of 190 mm and a thickness of 17 mm, and the acrylic triangular bracket (180 mm long, 130 mm wide, 1 mm high) is placed on it. An Animatics SmartMotor SM23165DT high-speed micro motor and a DLP PRO6500 high-speed projector are used. The CMOS camera is used to scan objects and adopts 3D Studio Max software to obtain the modeling image, as shown in Fig. 4.

Experiment 1: Reduce crosstalk to invisible to the naked eye

1. Speed of DLP: According to the rule of the 3D display, 240 Hz frames can reduce the crosstalk by fourfold compared with that for 60 Hz frames, so we chose a speed of 240 Hz for the DLP.
2. Number of cross-sectional views of 3D object: On the basis of Eq. (1), we chose angle δ as 15° (24 images).
3. Speed of DSM:
   (1) According to Lueder's suggestion[24] that an addressing circuit with a speed of four times the frame frequency should be adopted to reduce crosstalk, we preliminarily chose a motor speed of four times the frame rate of the DLP, namely 960 rpm, so that the speeds of the DSM and DLP could be matched. However, no stereoscopic imaging occurred, and only fuzzy and wobbly scenes were observed.
   (2) On the basis of Eq. (2), we set δ to 240 Hz, then the speed of the motor μ was 1000 rpm and the 3D scene vibrated. When the motor speed reached 1300 rpm, the surround effect

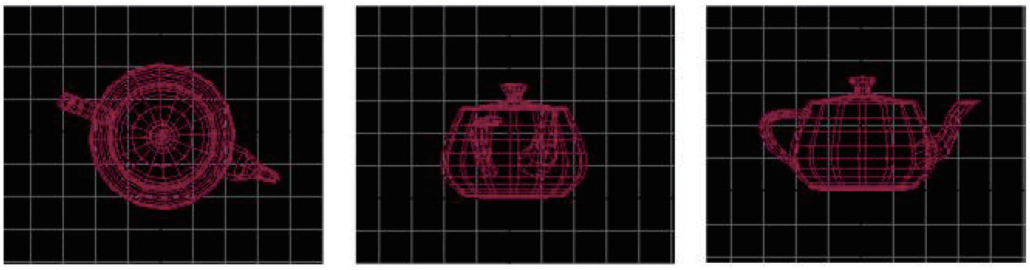

(a) (b) (c)

Fig. 4. (Color online) Modeling image. (a) Top, (b) back, and (c) front views.

appeared, and the 3D object rotated at a uniform and low speed. Then, when the motor speed reached 1704 rpm, the floating 3D object appeared smoothly above the rotating disc. However, when the motor speed was further increased, the display started to blur, rotate, and swing again.

Finally, when the motor speed was set at 1704 rpm, we were able to reduce the crosstalk and observe the objects suspended in the air. Figure 5 shows the 3D views from different angles.

Experiment 2: Make the hover display clearer

1. Different angles θ (60, 30, 15, and 10°) were selected using Eq. (2) without the ALSD. As shown in Fig. 6, the smaller the angle (i.e., the larger the number of images), the sharper the 3D scene will be. However, owing to the increase in the number of images, the performance and projection rate of DLP will increase correspondingly.

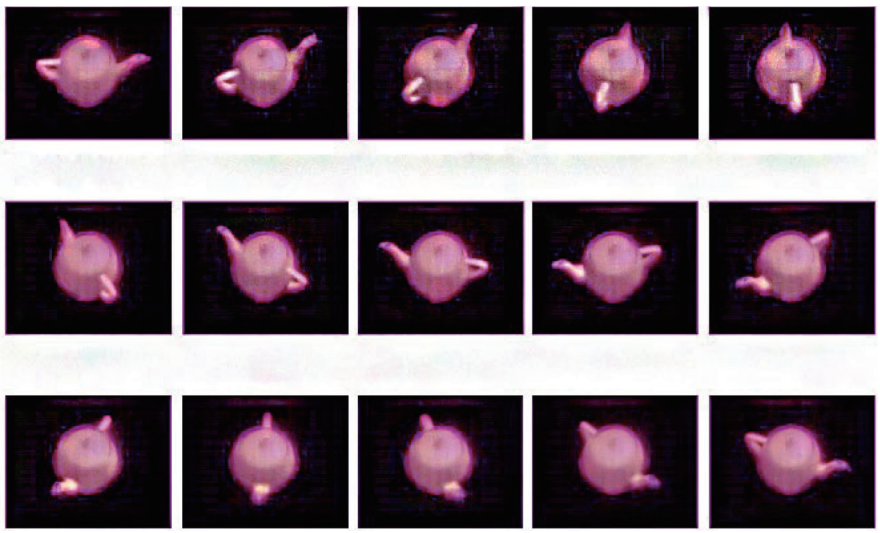

Fig. 5. (Color online) 3D views from different angles.

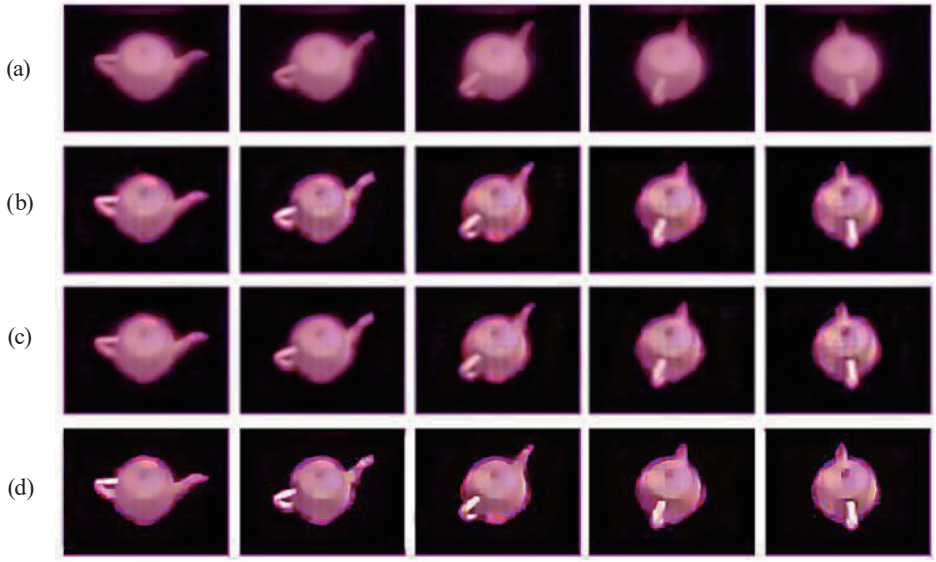

Fig. 6. (Color online) Cross-sectional views of 3D object with different angles. (a) 60°. (b) 30°. (c) 15°. (d) 10°.

Fig. 7. (Color online) Display results from different angles of ALSD. (a) 2°. (b) 1°. (c) 0.5°.

2. On the basis of the characteristics of the ALSD, an angle of 5° (72 pictures) was chosen with different ALSD angles (1, 0.5, and 2°). As shown in Fig. 7, 0.5° is the angle with the best display effect, but it is computationally expensive compared with an angle of 1°.

5. Conclusion

The proposed display system can enable the observer to observe 3D objects without wearing any equipment, and the whole set of equipment can be used repeatedly. In addition, compared with mainstream holographic 3D systems, such as those developed by Cambridge Enterprise[20] and Motohiro *et al*.,[21] this system is more practical and easily usable at a low cost. In particular, the definition and the observable angle of the RDSS are greatly improved due to the addition of the ALSD. Additionally, the RDSS overcomes the vibration problem when the motor rotates at high speeds. Overall, the RDSS has a small information requirement, low redundancy, and high speed, and produces clear images.

However, this system has various shortcomings. For example, the experimental results show that the theoretical data cannot eliminate crosstalk, possibly because the DSM had a large load on the rotating system.[26–28] In addition, owing to the limited amount of light field information, the display scene is transparent and lacks occlusion information,[29] so the observation should be in a dark environment. Furthermore, the observable range of the device is limited for human eyes, and the image display size is still limited.

The RDSS can be widely used in exhibitions, in advertisements, in the generation of medical images, and in modeling displays. In the future, we aim to develop real-time dynamic transmission control of the 3D display system.

Acknowledgments

This work was supported by the Ph.D. Start-Up Foundation of Longyan University, China (No. LB2020010), Longyan University's Qi Mai Science and Technology Innovation Fund Project of Liancheng [2018]132 and Shanghang 2019SHQM05 County, Longyan and Longyan

University's Research and Development Team Fund (2018)8, and the Great Project of Production, Teaching, and Research of Fujian Provincial Science and Technology Department (2019H6023).

References

1 E. Lueder: 3D Displays (John Wiley & Sons, Ltd., 2012) pp. 282–287. https://doi.org/10.1002/9781119962762
2 R. Patterson: J. Soc. Inf. Disp. **15** (2007) 861. https://doi.org/10.1889/1.2812986
3 D. Smalley, E. Nygaard, K. Squire, J. Van Wagoner, J. Rasmussen, S. Gneiting, K. Qaderi, J. Goodsell, W. Rogers, M. Lindsey, K. Costner, A. Monk, M. Pearson, B. Haymore, and J. Peatross: Nature **553** (2018) 486. https://doi.org/10.1038/nature25176
4 R. Hirayama, D. Martinez Plasencia, N. Masuda, and S. Subramanian: Nature **575** (2019) 320. https://doi.org/10.1038/s41586-019-1739-5
5 L. Luo, Q. H. Wang, Y. Xing, H. Deng, H. Ren, and S. Lia: Opt. Commun. **438** (2019) 54. https://doi.org/10.1016/j.optcom.2019.01.013
6 Y. Kakehi, M. Iida, T. Naemura, Y. Shirai, M. Matsushita, and T. Ohguro: IEEE Comput. Graphics Appl. **25** (2005) 48–53. https://doi.org/10.1109/MCG.2005.14
7 J. Liu, L. C. Cao, E. Stoykova, P. Ferraro, P. Memmolo, and P. A. Blanche: J. Opt. Soc. Am. A. **38** (2021) DH1–DH2. https://doi.org/10.1364/JOSAA.419210
8 S. Yoshida, S. Yano, and H. Ando: Trans. Virtual Reality Soc. Jpn. **15** (2010) 121.
9 M. M. Crenshaw: Arts (Basel) **8** (2019) 122. https://doi.org/10.3390/arts8030122
10 T. C. Ponn, Y. P. Zhang, and L. C. Cao: Appl. Sci. **10** (2020) 7057. https://doi.org/10.3390/app10207057
11 A. Jones, I. McDowall, H. Yamada, M. Bolas, and P. Debevec: ACM Trans. Graphics **26** (2007) 3. https://doi.org/10.1145/1276377.1276427
12 W. Hui: Three Dimensional Display of Wavefront Reconstruction (Science Press, Peking, 2017) pp. 7–39.
13 H. Wu, H. Jin, Y. Sun, Y. W, M. Ge, Y. Chen, and Y. F. Chi. BMC Ophthalmol. **16** (2016) 45. https://doi.org/10.1186/s12886-016-0223-3
14 G. J. Woodgate, D. Ezra, J. Harrold, N. S. Holliman, G. R. Jones, and R. R. Moseley: Signal Process. Image Commun. **14** (1998) 131. https://doi.org/10.1016/S0923-5965(98)00033-2
15 K. Choi, J. Kim, Y. J. Lim, and B. Lee. Opt. Express **13** (2005) 10494. https://doi.org/10.1364/OPEX.13.010494
16 H. Kimura, T. Uchiyama, and H. Yoshikawa: ACM SIGGRAPH 2006 Emerging Technol. (2006) 20-es. https://doi.org/10.1145/1179133.1179154
17 B. C. Zhao, R. Y. Huang, and G. J. Lv: Optik **226** (2021) 165691. https://doi.org/10.1016/j.ijleo.2020.165691
18 J. Geng: Adv. Opt. Photonics. **5** (2013) 456–535. https://doi.org/10.1364/AOP.5.000456
19 A. M. Beigzadeh, M. R. Rashidian Vaziri, and F. Ziaie: Nucl. Instrum. Methods Phys. Res., Sect. A **864** (2017) 40. https://doi.org/10.1016/j.nima.2017.05.019
20 University of Cambridge Enterprise: https://www.enterprise.cam.ac.uk/opportunities/360-3d-light-field-display/ (accessed April 2020).
21 M. Motohiro, S. Daisuke, and T. Hideaki: UIST '19: Proc. 2019 32nd Annual ACM Symp. User Interface Software and Technology (UIST, 2019) 625–637.
22 Y. Takeshi, M. Osamu, and Y. Hiroshi: Opt. Eng. **51** (2012) 7. https://doi.org/10.1117/1.OE.51.7.075802
23 R. Ng, M. Levoy, and M. Bredif: Pat Hanrahan Stanford Technol. Rep. (ICTSR, 2005) 1–11.
24 E. Lueder: 3D Displays (John Wiley & Sons, Ltd., 2012). https://doi.org/10.1002/9781119962762
25 T. A. Theoharis, A. R. L. Travis, and N. E. Wiseman: Comput. Graphics Forum **9** (1990) 337. https://doi.org/10.1111/j.1467-8659.1990.tb00425.x
26 C. Zhou, H. Li, and Y. Bian: Identifying the Optimal 3D Display Technology for Hands-On Virtual Experiential Learning: A Comparison Study (IEEE Access, 2020) pp. 73791–73803. https://doi.org/10.1109/ACCESS.2020.2988678
27 S. K. Nayar and V. N. Anand: Computer **40** (2007) 54. https://doi.org/10.1109/MC.2007.226
28 J. H. Lee, J. Park, D. K. Nam, S. Y. Choi, D. S. Park, and C. Y. Kim: Opt. Express. **21** (2013) 26820. https://doi.org/10.1364/OE.21.026820
29 H. Nakanuma, H. Kamei, and Y. Takaki: Proc. Stereoscopic Displays and Virtual Reality Systems XII (22 March 2005) 5664. https://doi.org/10.1117/12.589596